# Anomalous Impurity Segregation and Local Bonding Fluctuation in *l*-Si

G. Fisicaro,[1,*] K. Huet,[2] R. Negru,[2] M. Hackenberg,[3] P. Pichler,[3,4] N. Taleb,[5] and A. La Magna[1]
[1]*CNR IMM, Z.I. VIII Strada 5, I -95121 Catania, Italy*
[2]*Excico 13-21 Quai des Gresillons, 92230 Gennevilliers, France*
[3]*Fraunhofer Institute for Integrated Systems and Device Technology, Schottkystrasse 10, 91058 Erlangen, Germany*
[4]*Chair of Electron Devices, University of Erlangen-Nuremberg, Cauerstrasse 6, 91058 Erlangen, Germany*
[5]*Probion, 37 Rue de Fontenay, 92220 Bagneux, France*
(Received 12 September 2012; published 13 March 2013)

Anomalous impurity redistribution after a laser irradiation process in group-IV elements has been reported in numerous papers. In this Letter, we correlate this still unexplained behavior with the peculiar bonding character of the liquid state of group-IV semiconductors. Analyzing the B-Si system in a wide range of experimental conditions we demonstrate that this phenomenon derives from the non-Fickian diffusion transport of B in *l*-Si. The proposed diffusion model relies on the balance between two impurity states in different bonding configurations: one migrating at higher diffusivity than the other. This microscopic mechanism explains the anomalous B segregation, whereas accurate comparisons between experimental chemical profiles and simulation results validate the model.

DOI: 10.1103/PhysRevLett.110.117801 PACS numbers: 61.20.−p, 61.72.U−, 64.70.D−

The tendency to form directional bonds makes Si an intriguing material when its liquid phase is considered. Liquid Si (*l*-Si) is a metal with electrical and optical properties comparable to other Lennard-Jones metals (e.g., *l*-Al), but with a coordination number ~6, much lower than that ~12 predicted by (dynamic) close packing arguments. It is now well understood that the low coordination number of *l*-Si is related to the persistence of covalent bonds in the liquid phase, predicted by atomistic simulations [1], and recently evaluated by Compton scattering measurements [2]. The persistence of bonds with tetrahedral character in the liquid phase has also been consistently related to a series of thermodynamic anomalies (density increase upon melting, nonlinear dependence on temperature $T$ of density and heat capacity) of *l*-Si and other liquids like *l*-Ge and water.

The emerging scenario for the atomic structure of *l*-Si is the coexistence between the conventional liquid metal states with locally covalently bounded regions which are continuously formed and dissolved in short time scales. The temperature dependence of the average fraction of these fluctuating covalent bonds causes the anomalous thermodynamic properties of *l*-Si [3].

The question arises whether local bonding fluctuations also affect mass transport in *l*-Si such as self-diffusion and/or impurity diffusion. *Ab initio* simulations [4] estimate a strong decrease of the Si self-diffusion coefficient from $2.73 \times 10^{-4}$ cm$^2$/s to $6.2 \times 10^{-6}$ cm$^2$/s for the changeover from the stable liquid to the undercooled regime. This prediction has not yet been proved experimentally and even less is known on the mechanisms of impurity diffusion in *l*-Si.

Anomalies of impurity redistribution have been commonly observed in Si and Ge that undergo a melting laser process. A melting process by laser thermal annealing (LTA) for a time scale of sub-$\mu$s is expected to produce boxlike impurity profiles after a liquid-phase epitaxial recrystallization of the molten region. This expectation relies on the high impurity diffusivity in *l*-Si, which is about eight orders higher than that in solid Si [5] and on the $k \sim 1$ solid-liquid segregation coefficient of some III and V group elements such as B, P, and As [6]. In fact, the experimental impurity profile is usually significantly different from that predicted. A strong dopant pileup is commonly observed close to the melt depth region [7,8]. In this Letter, we propose a two-state diffusion model that accurately describes experimental B profiles obtained after LTA. The presence of two B states in *l*-Si is consistent with the atomic structure of *l*-Si.

We have experimentally studied the B redistribution in Si due to LTA processes in a rather wide range of conditions. Laser irradiations have been performed in an implanted Silicon substrate (B 3 keV energy, $5 \times 10^{14}$ cm$^{-2}$ dose, black circles in the figures). The samples have been annealed using the EXCICO LTA system ($\lambda = 308$ nm) at room temperature, with a pulse duration of 160 ns and a frequency of 1 Hz for multishot annealing. Laser energy densities of 2.0, 2.3, 2.6 J/cm$^2$ have been considered in single and multipulse configurations. After implantation and/or LTA, all samples remain monocrystalline, as verified by transmission electron microscopy. Chemical B profiles have been analyzed by means of secondary ion mass spectroscopy (SIMS).

Figure 1 reports an example of anomalous impurity redistribution after LTA. The anomaly refers to the apparent against-gradient diffusion process which, as it will be discussed in the following, cannot be modeled by means of the Fickian diffusion equation and the conventional segregation effects ($k \leq 1$) at the $l - s$ interface.

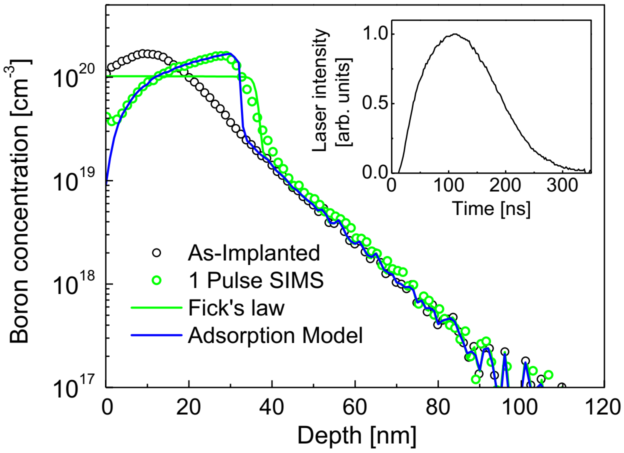

FIG. 1 (color online). SIMS (green circles) and simulated (solid lines) $B$ profiles obtained after a post-implantation laser irradiation at 2.0 J/cm$^2$. Results obtained with Eqs. (1) and (2) are reported as green and blue lines, respectively. In the inset the laser pulse is plotted.

In a first attempt, we simulate the B transport during laser irradiation coupling the Fickian diffusion equation for the B concentration $C_B$

$$\frac{\partial C_B}{\partial t} = \nabla[D_B(T, \Phi)\nabla C_B], \tag{1}$$

with a model [9] for the Stephan problem. This model predicts the time evolution of the thermal field $T$ and the liquid-solid boundary. The latter can be evaluated within the phase-field approach by means of a phase function $\Phi$ which takes different values in the liquid and solid regions [10,11]. In Eq. (1), $D_B(T, \Phi)$ is the temperature- and phase-dependent diffusivity of boron. The discrepancy between the simulated and the measured density profile is significant (see Fig. 1 green solid line). The resulting boxlike profile predicted by this simplified model is essentially due to the jump of the diffusivity in the liquid $D_{B\mathrm{liq}} = 2.4 \times 10^{-4}$ cm$^2$/s [5] and solid phase $D_{B\mathrm{sol}} = 0.87\exp(\frac{-3.46\mathrm{eV}}{k_B T})$ cm$^2$/s [12]. The temperature field has been simulated according to the approach described in Refs. [11,13] using the experimental laser pulse shown in the inset of Fig. 1. At the irradiated surface, an outgoing heat flux proportional to $T^4$ has been implemented while the room temperature $T = 300$ K has been fixed on the outer surface of the wafer.

The extension of the diffusion model Eq. (1), that considers the segregation effect at the $l - s$ interface [13,14] and the inclusion of the thermodiffusion, does not describe the experimental results [15]. Indeed, in these case the segregation coefficient, determining the ratio of the impurity density at the solid and liquid sides of the interface, varies within the range $k_0 < k(v) < 1$; where $k_0$ is the equilibrium value and $k(v)$ grows with $l - s$ interface speed $v$ and asymptotically reaches the limit 1 value when $v >> 1$ m/s. As a consequence, by varying the process conditions, the simulated profiles show no significant segregation or the conventional segregation peak at the irradiated surface. The latter peak is usually visible if $k_0$ is small (e.g., $k_0 < 0.1$).

Ong *et al.* report [8] that the anomalous segregation can be qualitatively described by a position dependent $k(x)$ segregation coefficient where $k$ takes the equilibrium value $k_0$ at the very beginning of the re-solidification, then increases to a value $k_{\mathrm{trans}} > 1$ in a transient stage and returns to a value $k \leq 1$ until the solidification is completed. These qualitative features can be simulated using the diffusion-segregation equation developed by You *et al.* [16]:

$$\frac{\partial C_B}{\partial t} = \nabla\left[D_B(T, \Phi)C_{\mathrm{eq}}(\Phi)\nabla\frac{C_B}{C_{\mathrm{eq}}(\Phi)}\right], \tag{2}$$

with $C_{\mathrm{eq}}(\Phi)$ denoting a phase-dependent equilibrium concentration. $C_{\mathrm{eq}}(\Phi)$ defines the ratio of the equilibrium concentrations of boron in the different phases. Taking a value of 1 in the liquid, we assume a value of $C_{\mathrm{eq}} = k_0(B) = 0.8$ in the solid to model equilibrium segregation [17]. To reproduce adsorption, a 1 nm thick adsorption layer is defined at the $l - s$ interface with a value of $C_{\mathrm{eq}} > 1$. Note that this correction promotes a positive impurity flux toward the $l - s$ interface. The values of $C_{\mathrm{eq}}$ and $D_B$ in the adsorption layer were used as fitting parameters. The simulation result shown in Fig. 1 was obtained with $D_B = 1.8 \times 10^{-7}$ cm$^2$/s and $C_{\mathrm{eq}} = 1.9$ in the adsorption layer.

Although the model of [Eq. (2)] or similar formulations can fit the impurity profiles for a particular process using proper choices of the segregation coefficients, the microscopic mechanism causing this anomalous segregation kinetics of B and other impurities is not known. We hypothesize that the waterlike anomalies of the bonding in *l*-Si make unreliable the Fick-law scenario for the impurity diffusion in *l*-Si. In particular, we speculate that the balance between the covalent and metallic local bond states as a function of $T$ in liquid phase is responsible for the adsorption behavior of the $l - s$ boundary, which practically acts as an impurity sink. In order to bring a stronger supporting argument to this hypothesis, we propose a modified B diffusion model which is consistent with the *l*-Si atomic structure [3].

In our model, we consider the effects of the bonding state of *l*-Si on the B migration mechanism; therefore, we assume in analogy that B atoms can coexist in two different states, one highly mobile and the other slowly diffusing. The mobile state is virtually bounded to the metallic zones while the low diffusivity state is trapped by those Si atoms forming covalent bonds. The temperature affects the corresponding concentrations as the persistence of covalent bonding depends on $T$ and becomes more relevant in undercooled *l*-Si. As a consequence, we model the balance between the two states by means of rate equations where rate parameters are $T$ dependent. The model reads

$$\frac{\partial C_B}{\partial t} = \frac{\partial C_B^{\mathrm{HD}}}{\partial t} + \frac{\partial C_B^{\mathrm{LD}}}{\partial t}, \tag{3}$$

$$\frac{\partial C_B^{\mathrm{HD}}}{\partial t} = \nabla[D_B^{\mathrm{HD}} \nabla C_B^{\mathrm{HD}}] + k^{\tau}(C_B^{\mathrm{LD}} - \bar{R} C_B^{\mathrm{HD}}), \tag{4}$$

$$\frac{\partial C_B^{\mathrm{LD}}}{\partial t} = \nabla[D_B^{\mathrm{LD}} \nabla C_B^{\mathrm{LD}}] - k^{\tau}(C_B^{\mathrm{LD}} - \bar{R} C_B^{\mathrm{HD}}), \tag{5}$$

where $D_B^{\mathrm{HD}}$ and $D_B^{\mathrm{LD}}$ are the diffusivity of boron atoms in the higher and lower diffusivity state in the liquid phase. $C_B^{\mathrm{HD}}$ and $C_B^{\mathrm{LD}}$ are the corresponding concentrations. $k^{\tau}$ is a rate coefficient ruling the transition between the two B states which should be also related to the rapidity of the bonding order fluctuations in $l$-Si. Its value was fixed as a constant (not null in the melting phase). $\bar{R}(T)$ is the average (equilibrium) ratio between low and high diffusivity states at constant $T$. When dopant atoms in the lower diffusivity state are strongly favored (i.e., undercooled regions), $\bar{R}(T) > 1$, while $\bar{R}(T) < 1$ when atoms in the higher diffusivity state characterize the impurity kinetics (i.e., stable liquid regions). In the solid phase, metallic bonds are not present and $D_{B\mathrm{sol}} = D_{B\mathrm{sol}}^{\mathrm{HD}} = D_{B\mathrm{sol}}^{\mathrm{LD}}$ [18].

The designed experiment allows us to follow the dopant evolution in the wide range of conditions, from shallower melting processes to deeper ones, necessary for getting a reliable calibration of $k^{\tau}$ and $\bar{R}(T)$. Solid lines in Fig. 2 represent the simulated $B$ dopant redistribution after one pulse laser irradiations for all the processed samples. A satisfying agreement can be found for the against-gradient, pileup and no-pileup regime. The calibration procedure gives the value of $k^{\tau} = 1.0 \times 10^7\ \mathrm{s}^{-1}$ for the reaction rate, while in the inset of Fig. 2 the $\bar{R}(T)$ is shown. The limit values of $\bar{R}(T)$ in the deep undercooled and overheated regimes are 50.0 and 0.4, respectively. $\bar{R}(T)$ switches from 50.0 to 0.4 in a ~10 K wide region close to the melting point.

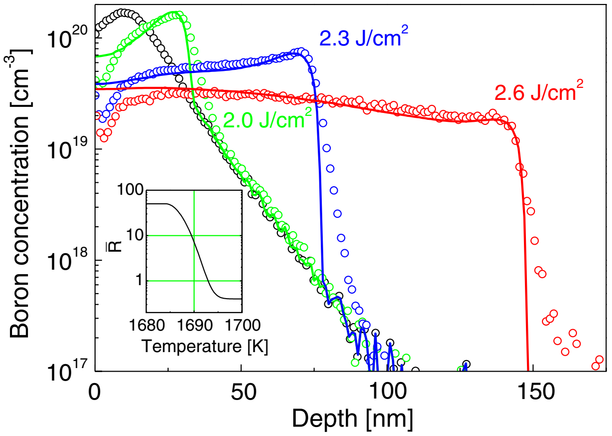

FIG. 2 (color online). SIMS (circles) and simulated (two-state model Eqs. (3)–(5), solid lines) $B$ profiles obtained after single pulse laser irradiations at 2.0 (green), 2.3 (blue), and 2.6 (red) J/cm$^2$ energy densities. The inset shows the $\bar{R}(T)$ function described in the text.

The extracted high temperature value $\bar{R}(T) = 0.4$ is in agreement with the work of Štich *et al.* [1] which predicts, by means of molecular dynamics simulations of molten Si, a ratio of covalent and metallic bonds ~0.42 in $l$-Si at a temperature greater than the Silicon melting point. The $l$-Si boron diffusivity in the high (low) diffusivity state was found to be $D_B^{\mathrm{HD}} = 3.3 \times 10^{-4}[\mathrm{cm}^2/\mathrm{s}]$ ($D_B^{\mathrm{LD}} = 6.6 \times 10^{-5}[\mathrm{cm}^2/\mathrm{s}]$). Note that the experimental value of the B diffusivity in the $l$-Si $D = 2.4 \times 10^{-4}\ \mathrm{cm}^2/\mathrm{s}$ [5] is recovered by our two-state model in the case of a fixed uniform (in the space) ratio of the two components. All the simulation results obtained with the model Eqs. (3)–(5), has been carried out with the unique parameter setting reported above. The tolerance of the parameter fitting is ~5% (except for $k^{\tau}$ which spreads between $0.5 \times 10^7[\mathrm{s}^{-1}]$ and $1.5 \times 10^7[\mathrm{s}^{-1}]$). Outside this tolerance the calibrated model fails in quantitatively recovering our experimental data.

The decrease of the average boron diffusion in the undercooled liquid state, which has been carried out from our modeling, appears similar to that extracted for $l$-Si self-diffusion in the work of Jakse *et al.* [4]. In this case, by means of *ab initio* molecular dynamics simulations they estimated a decrease of the Si self-diffusion coefficient in the undercooled state being 40 times lower than in the stable liquid. Although they investigated the deep undercooled regime, their work can suggest the degree of impact on the mass transport characteristic of the undercooled state when collective displacements of the tetrahedral network appear. Note that these comparisons have to be considered as qualitative indications. Indeed, the Si self-diffusion evaluation in the liquid phase reported in Ref. [4] has been performed in the case of pure Si. The impurity presence could substantially modify the local ratio of the metallic and covalent bonds and, as a consequence, the quantitative estimation of any transport coefficient and its dependence on the temperature.

Temperature-dependent bulk diffusivity is one direct consequence of the two-state model. However, the anomalous segregation behavior cannot be explained only by means of this dependence for the dopant average diffusivity in the liquid phase being the impurity pileup mechanism inherently related to the local imbalance between states with high and low mobility. In order to clarify this issue, snapshots of the dopant evolution have been reported in Fig. 3 for the 2.3 J/cm$^2$ laser fluence case. The temperature dependence on the position (Fig. 3 green solid line) helps to follow the different evolution stages in undercooled and nonundercooled $l$-Si.

During a melting laser annealing process, boron atoms are in two different states with different mobilities. In particular, dopant atoms in the lower diffusivity state are

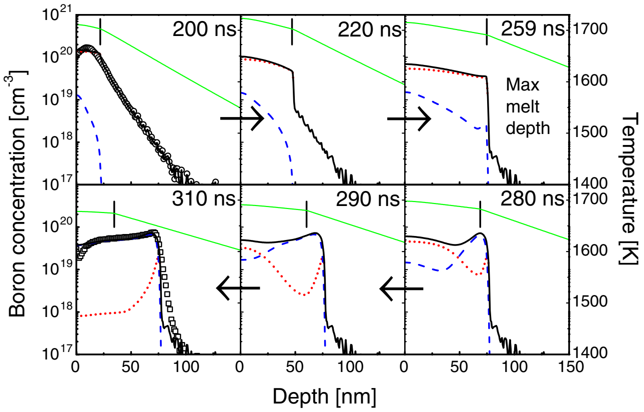

FIG. 3 (color online). Dopant evolution during the laser irradiation process (2.3 J/cm$^2$). Melting (regrowth) stage is indicated by the forward (backward) arrow. We plot the total (black solid line), the HD (red dot), and the LD (blue dash) boron concentrations. The as-implanted (empty circles) and the final (empty squares) SIMS profiles are also shown, as well as the local temperature (green line) and the $l - s$ interface (bar).

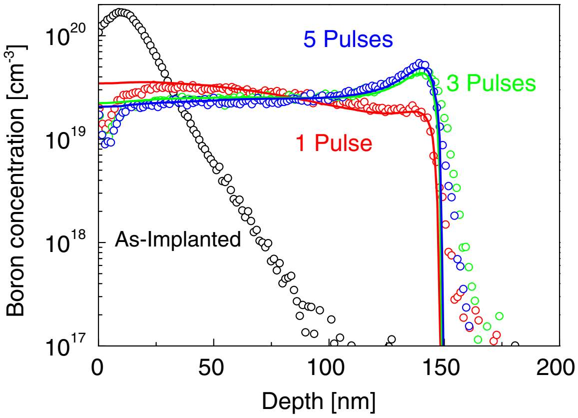

FIG. 4 (color online). Experimental (circles) and simulated (lines) dopant redistribution in the melting phase in implanted Si after multipulse laser irradiation (2.6 J/cm$^2$).

strongly favored in regions of low temperature (i.e., undercooled regions), while atoms in the higher diffusivity state characterize the impurity kinetics in the stable liquid regions. For a laser irradiation with a maximum melt depth greater than the dopant region, during the melting stage (upper panels of Fig. 3), the majority of the dopant atoms (71%) resides in their high diffusivity state as the temperature is significantly above the Silicon melting point. After the maximum melt depth is reached, during regrowth, the dopant atoms are shifted towards the solid-liquid interface (lower panels of Fig. 3, blue lines), due to the presence of the undercooled phase which favors the $B$ state with low diffusivity and a large density gradient of the high diffusivity component (red lines). As a consequence, a net migration of impurity atoms from left to right (in the panel) is the combined result of the two-component evolution.

Depending on the laser fluence, i.e., on the maximum melt depth of the process, different final distributions can be achieved in the one pulse case, as shown in Fig. 2. For lower fluence (green line) the anomaly of the dopant redistribution is more pronounced (against-gradient regime), while it becomes less important as the melt depth increases (pileup, blue line) until pileup is not evidenced anymore for larger fluence (red line). The two-state diffusivity model reproduces carefully the profile shape for any value of the fluence (melt depth).

When the laser fluence is fixed and the sample is processed with multipulse irradiation, a dopant accumulation near the maximum melt depth is experimentally observed [7], which saturates after a certain number of pulses. Our model also reproduces this phenomenon. Figure 4 shows simulation results relative to dopant redistribution in the melting phase after multipulse irradiations. In this case, during the first pulse boron atoms have sufficient time to diffuse deeply throughout the molten region, but not enough to form the pileup at the maximum melt depth. In the subsequent pulse (second pulse) the starting distribution of boron atoms is flat and additional impurities are displaced much closer to the maximum melt depth. Consequently, they can accumulate and form the peak. The boron pileup saturation after a certain number of pulses is related to the achievement of a quasiequilibrium condition between the laser process variables and the characteristic kinetics and reactions of the involved constituents. The data of Fig. 4 refer to LTA with a laser fluence of 2.6 J/cm$^2$ and after a number of pulses from 1 to 5. The good agreement observed between the SIMS and the simulation for single and multishot conditions confirms the validity of the two-state diffusivity model for the Boron evolution in $l$-Si and the role played by the undercooled liquid.

In conclusion, we have demonstrated that the anomalous impurity redistribution in Si during a LTA process derives from a unique diffusion mechanism which is at the basis of all the observed features. The model is consistent with the peculiar properties of $l$-Si, i.e., the coexistence between the covalent and metallic bonds, and reproduces the experimental data for all the studied regimes by varying laser fluence and number of shots. Future investigations will be devoted to infer quantitative relations between the relative abundance of the diffusion states of the impurity at different temperatures and the measurable ratio between covalent and metallic bonds in $l$-Si [2]. Moreover, the similarity of the bond network of liquid and amorphous Si indicates the possibility of non-Fickian impurity diffusion also in $\alpha$-Si (see, e.g., Ref. [19]). However, since $\alpha$-Si is solid, a model extension is needed in this case.

The research leading to these results has received funding from the European Seventh Framework Programme (No. FP7/2007-2013) under Grant Agreement No. 258547 ATEMOX (Advanced Technology Modeling for Extra-Functionality Devices).

*giuseppe.fisicaro@imm.cnr.it

[1] I. Štich, R. Car, and M. Parrinello, Phys. Rev. Lett. **63**, 2240 (1989).

[2] J. T. Okada, P. H.-L. Sit, Y. Watanabe, Y. J. Wang, B. Barbiellini, T. Ishikawa, M. Itou, Y. Sakurai, A. Bansil, R. Ishikawa, M. Hamaishi, T. Masaki, P.-F. Paradis, K. Kimura, T. Ishikawa, and S. Nanao, Phys. Rev. Lett. **108**, 067402 (2012).

[3] H. Tanaka, Phys. Rev. B **66**, 064202 (2002).

[4] N. Jakse and A. Pasturel, Phys. Rev. B **79**, 144206 (2009).

[5] H. Kodera, Jpn. J. Appl. Phys. **2**, 212 (1963).

[6] R. F. Wood, C. W. White, and R. T. Young, in *Semiconductors and Semimetals*, edited by R. K. Willardson and A. C. Beer, Vol. 23 (Academic, New York, 1984), pp. 251–312.

[7] E. V. Monakhov, B. G. Svensson, M. K. Linnarsson, A. La Magna, M. Italia, V. Privitera, G. Fortunato, M. Cuscunà, and L. Mariucci, Appl. Phys. Lett. **87**, 192109 (2005).

[8] K. K. Ong, K. L. Pey, P. S. Lee, A. T. S. Wee, X. C. Wang, and Y. F. Chong, Appl. Phys. Lett. **89**, 172111 (2006).

[9] A. W. Date, Int. J. Heat Mass Transfer **34**, 2231 (1991).

[10] A. Karma and W.-J. Rappel, Phys. Rev. E **57**, 4323 (1998).

[11] K. Huet, G. Fisicaro, J. Venturini, H. Besaucèle, and A. La Magna, Appl. Phys. Lett. **95**, 231901 (2009).

[12] P. M. Fahey, P. B. Griffin, and J. D. Plummer, Rev. Mod. Phys. **61**, 289 (1989).

[13] A. La Magna, P. Alippi, V. Privitera, G. Fortunato, M. Camalleri, and B. Svensson, J. Appl. Phys. **95**, 4806 (2004).

[14] A. A. Wheeler, W. J. Boettinger, and G. B. McFadden, Phys. Rev. A **45**, 7424 (1992).

[15] M. Hackenberg, K. Huet, R. Negru, J. Venturini, G. Fisicaro, A. La Magna, and P. Pichler, in *Ion Implantation Technology*, edited by L. Pelaz, I. Santos, R. Duffy, F. Torregrosa, and K. Bourdelle, AIP Conf. Proc. No. 1496 (AIP, New York, 2012), p. 241.

[16] H. M. You, T. Y. Tan, U. M. Gösele, S.-T. Lee, G. E. Höfler, K. C. Hsieh, and J. N. Holonyak, J. Appl. Phys. **74**, 2450 (1993).

[17] F. Trumbore, Bell Syst. Tech. J. **39**, 205 (1960).

[18] Due to the small time scale of the process, the overall diffusion of B in the solid region is negligible and we do not include it in the model of the details of the defect driven diffusion mechanism of B in solid *c*-Si (see, e.g., Ref. [12]).

[19] S. Mirabella, D. De Salvador, E. Bruno, E. Napolitani, E. F. Pecora, S. Boninelli, and F. Priolo, Phys. Rev. Lett. **100**, 155901 (2008).